Flexible and Green Electronics Manufactured by Origami Folding of Nanosilicate-Reinforced Cellulose Paper

Kadumudi, Firoz Babu; Trifol, Jon; Jahanshahi, Mohammadjavad; Zsurzsan, Tiberiu Gabriel; Mehrali, Mehdi; Zeqiraj, Eva; Shaki, Hossein; Alehosseini, Morteza; Gundlach, Carsten; Li, Qiang

Total number of authors:
15

Published in:
ACS Applied Materials and Interfaces

Link to article, DOI:
10.1021/acsami.0c15326

Publication date:
2020

Document Version
Peer reviewed version

Flexible and green electronics manufactured by origami folding of nanosilicate-reinforced cellulose paper

Firoz Babu Kadumudi[1], Jon Trifol [2], Mohammadjavad Jahanshahi[3,4] , Tiberiu - Gabriel Zsurzsan[5], Mehdi Mehrali[6,7], Eva Zeqiraj[8], Hossein Shaki[1,9], Morteza Alehosseini[1], Carsten Gundlach[8] , Qiang Li [10,11], Mingdong Dong[10], Mohsen Akbari[12,13], Arnold Knott[5]. Kristoffer Almdal[14], Alireza Dolatshahi-Pirouz[6,15,*]

[1]Department of Health Technology, Technical University of Denmark (DTU), 2800 Kgs. Lyngby, Denmark.

[2]Danish Polymer Center, Department of Chemical Engineering, Technical University of Denmark (DTU), 2800 Kgs. Lyngby, Denmark

[3]Student Research Committee, School of Medicine, Bam University of Medical Sciences, 4340847 Bam, Iran.

[4]Department of Marine Chemistry, Faculty of Marine Science, Chabahar Maritime University, Chabahar, Iran

[5]Department of Electrical Engineering, Technical University of Denmark, 2800 Kgs. Lyngby Denmark

[6]Department of Health Technology, Institute of Biotherapeutic Engineering and Drug Targeting, Center for Intestinal Absorption and Transport of Biopharmaceuticals, Technical University of Denmark, Lyngby, 2800 Kgs, Denmark.

[7]Department of Mechanical Engineering, Technical University of Denmark, 2800, Kgs, Lyngby, Denmark

[8]Department of Physics, DTU Physics, Technical University of Denmark, 2800 Kgs. Lyngby, Denmark

[9]Biomedical Engineering Division, Faculty of Chemical Engineering, Tarbiat Modares University, P.O.Box: 14115-111, Tehran, Iran.

[10]Interdisciplinary Nanoscience Centre, Aarhus University, 8000 Aarhus, Denmark.

[11]School of Chemistry and Chemical Engineering, Shandong University, 250100 Jinan, China.

[12]Laboratory for Innovations in MicroEngineering (LiME), Department of Mechanical Engineering, University of Victoria, Victoria, BC V8P 5C2, Canada

[13]Center for Advanced Materials and Related Technologies (CAMTEC), University of Victoria, Victoria, BC V8P 5C2, Canada

[14]Department of Chemistry, Technical University of Denmark (DTU), 2800 Kgs. Lyngby, Denmark.

[15]Radboud university medical center, Radboud Institute for Molecular Life Sciences, Department of Dentistry - Regenerative Biomaterials, Philips van Leydenlaan 25, 6525EX Nijmegen, The Netherlands

*Correspondence should be addressed to Prof. A. Dolatshahi-Pirouz -aldo@dtu.dk.

Abstract

Today's consumer electronics are made from non-renewable and toxic components. They are also rigid, bulky, and manufactured in an energy-inefficient manner via CO_2 generating routes. Though petroleum-based polymers such as polyethylene terephthalate (PET) and polyethylene naphthalate (PEN) can address the rigidity issue; they have a large carbon footprint and generate harmful waste. Scalable routes for manufacturing electronics that are both flexible and eco-friendly (Fleco) could address the challenges in the field. Ideally, such substrates must incorporate into electronics without compromising device performance. In this work, we demonstrate that a new type of wood-based (Nanocellulose) material made via nanosilicate reinforcement can yield flexible electronics that can bend and roll without loss of electrical function. Specifically, the nanosilicates interact electrostatically with nanocellulose to reinforce thermal and mechanical properties. For instance, films containing 34 wt% of nanosilicate displayed an increased young modulus (1.5 times), thermal stability (290→310 ^{o}C), and a low coefficient of thermal expansion (CTE, 40 ppm/K). These films can also easily be separated and renewed into new devices through simple and low-energy processes. Moreover, we used very cheap and environmental friendly nanocellulose from American Value Added Pulping (AVAP®) technology, American Process and therefore, the manufacturing cost of our nanosilicate-reinforced nanocellulose paper is much cheaper ($0.016 per dm^{-2}) than many conventional polymer based substrates. Looking forward, the methodology highlighted herein is highly attractive as it can unlock the secrets of Flexible and Ecofriendly (Fleco) electronics and transform otherwise bulky, rigid, and "difficult-to-process" rigid circuits into more aesthetic and flexible ones, while simultaneously bringing relief to an already-overburdened ecosystem.

Key words: Nanocellulose, origami electronics, green electronics, flexible electronics, nanosilicate, circular economy

Introduction

Rapid technological advances in recent years have transformed our civilization into one dominated by electronics. Imagine, for a second, a world without portable devices, computers, mobile phones, televisions, and cameras; it sounds terrifying, right? Yet what is even more worrisome is the significant decrease in the lifetimes of consumer electronics. On average, many of the abovementioned devices are used for less than three years before they are discarded and replaced by new ones.[1-2] Have you ever stopped to think about what happened to your old smartphone or tablet ... or television set, for that matter? Likely, parts from your discarded phone are still lying around in a landfill not far from you—a ticking environmental bomb not only for your community but also for your health and the well-being of those you care about. Indeed, in the US alone, 426,000 cell phones and 112,000 computers were thrown away daily in 2007.[3] Obviously, this is not a sustainable scenario and it must be stopped before humanity enters a future consisting of inhabitable environments. On the other hand, the interest toward flexible electronics has increased enormously since they are bendable, conformable and can become readily utilized in wearable electronics.[4-6] The substrates used for these flexible electronics mostly rely on toxic and non-degradable petroleum-based polymers such as polyethylene terephthalate (PET) and polyethylene naphthalate (PEN).[7-8] This battle, in the author's opinions, begins with finding a replacement for conventional petroleum-based electronic substrates, which, despite their low cost and exciting properties, are very difficult to dispose of in an eco-friendly manner.[9-11]

To prevent this dystopia from occurring, Fleco materials such as cellulose, silk, starch, chitosan, collagen, and polylactic acid (PLA) are currently being explored as alternatives.[3, 12-15] Notably, these materials are all retrieved from renewable feedstock that is abundant, scalable, and low-cost. Perhaps one of the most promising candidates out of many

is nanocellulose (NC) derived from wood, as it is lightweight, non-toxic, flexible, recyclable, green, mechanically strong, and thermally stable.[3, 9-10] Because of this, NC can compete with conventional man-made materials such as metals, ceramics, alloys, glass, and plastics. Indeed, NC can display a coefficient of thermal expansion (CTE) as low as (0.1 ppm/K), with an estimated strength that is almost five times that of steel.[16] With around 30% of the landmass on planet earth being covered by forests, it is beyond a doubt that wood and its derivatives are the most abundant naturally derived materials at our disposal.[10, 17-18] Additionally, the abundance and amazing properties of such materials allow them to readily reunite with Mother Nature without giving rise to harmful waste products. Wood itself is also a carbon-neutral material that does not give rise to any net CO_2 release into the environment, in contrast to conventional petroleum-based polymers such as PET and PEN.[10]

Despite the many attractive qualities of NC and the vast annual cellulose production ($10^{11} – 10^{12}$ tons annually),[19] NC is, unfortunately, still far from actualizing its full potential, mostly because the current manufacturing schemes are either energy-consumptive ($4/lb., 2000 kWh/MT) or very expensive ($100/lb., 570 kWh/MT).[20] In comparison, the production prices of metallic materials such as aluminum and steel are $0.98/lb. and $2.38/lb., respectively. For this reason, it is obvious that conventional NC does not yield economically efficient routes for down-stream applications. Here, we have addressed this grand challenge in the field by using NC procured from a new methodology (American Value Added Pulping (AVAP®) technology, American Process), as it is capable of delivering highly crystalline, mechanically strong, thermally conductive, and stable NC at a cost-effective price compared to petroleum-based polymers (<$1/lb., 500 kWh/MT). This methodology also uses low energy, releasing less CO_2 than conventional NC production pipelines.[20-21]

Though AVAP® NC circumvents the cost-competitive, CO_2-generating, and energy-consumptive challenges associated with traditional manufacturing schemes, the reader will soon bear witness to the fact that substrates made from AVAP® NC could, according to our results, be less flexible and exhibit poorer dimensional stability at high temperatures than its more expensive counterparts. This is rather unfortunate, as foldability and high dimensional stability at elevated temperatures are key factors in ensuring the uncomplicated and continuous processing of substrates during the production of electronic devices. In particular, substrates that are difficult to handle and that are not foldable in a cyclic manner will disrupt the continuous roll-to-roll processing typically used to manufacture non-rigid electronics.[22-23]

Correspondingly, several emerging studies have shown that nanosilicate reinforcement can remedy the limitations imposed by several polymers—both natural and synthetic ones. Notably, the nanosilicate materials are non-toxic, easy to recycle, and scalable. Even at small amounts, they can facilitate a wide range of functionalities, such as increased mechanical strength, improved barrier properties, thermal stability, fire-resistance, and biological properties, into otherwise mono-functional materials. For these reasons, they have been extensively used in various scientific disciplines including biomedical engineering, medicine, material science, and mechanical engineering.[24-27]

This study demonstrates that the abundant and cheap AVAP® NC in combination with the nanosilicate Laponite® RD can yield flexible, strong, transparent, thermally stable, and easy-to-process NC paper that is similar to conventional NC, though at a much lower cost. It is, therefore, capable of addressing the abovementioned limitations through a simple, eco-friendly, scalable, and low-cost “one-pot” mixing procedure. For this reason, nanosilicate-reinforced AVAP® NC has the potential to conquer markets traditionally dominated by synthetic and non-recyclable materials such as plastics, glass, and metals.

Specifically, we have used these alternative electronic substrates to manufacture 3D-integrated circuits capable of complex electronic operations through paper origami. We have demonstrated that the developed origami circuits function in an uncompromised manner even after being bent 180°, folded, and rolled extensively. Notably, we were able to separate metallic circuits from the devices in a recyclable and ecofriendly manner using low-cost, non-toxic, and scalable methodologies. In summary, the present work adds another dimension to the development of Fleco materials, while opening doors into the realm of origami-based 3D integrated circuits (Figure 1).

Results

The forests have since ancient times been one the most generous supplier of support materials, tools and fuels to our civilization. Besides being recyclable and degradable lumber, paper, cellulose and nanofibrillated cellulose (NC) extracted from threes provide a wide range of exciting properties ranging from excellent mechanical, barrier and thermal properties. NC consists of high-aspect ratio fiber bundles of polysaccharides with a diameter that ranges between 4-20 nm and a length < 1 μm. Despite being considerably cheaper with a substantially smaller CO_2 footprint than more traditional NC variants, the AVAP® NC paper that we have manufactured in this study display somewhat inferior properties to these. We demonstrated that our casted AVAP® NC paper (both hot pressing and solvent casting) were less flexible, with a lower young modulus and higher coefficient of thermal expansion (CTE) than traditional NC paper. This prompted us to reinforce the paper with another low-cost and sustainable material, namely nanosilicate Laponite® RD from BYK additives to generate Lapolose. Laponite® RD is a dual-charged two-dimensional (2D) nanosilicate with a negative surface charge and a positive rim charge. Its chemistry is based on layered silica tetrahedral units with octahedral magnesia sheets and traces of lithium atoms (Chemical formula: $Na_{0.7}Si_8Mg_{5.5}Li_{0.3}O_{20}(OH)_4$)). In the following two sections, we will characterize

Lapolose in terms of transparency, water-barrier, thermal and mechanical properties and demonstrate that nanosilicate incorporation can bridge the current gap between the NC films developed herein and the others reported in the literature.

Lapolose Characterization

Figure 2a depicts the preparation of nanosilicate-reinforced nanocellulose (Lapolose) paper. In brief, nanocellulose was mixed with 2D nanosilicates to yield core-shell plates that were subsequently either hot-pressed or solvent-casted into thin paper films. Following the solvent evaporation process, layer-by-layer structures consisting of the core-shell plates were formed. The structures resembled the highly hierarchical mineral phase of nacre. To validate this hypothesis, we turned to X-ray diffraction (XRD) analysis to determine the intercalation of nanocellulose between the basal sheets of the 2D nanosilicate (Figure 2b), since fully intercalated and dispersed nanomaterials are needed to facilitate such nacre-mimetic structures. The XRD pattern for the nanosilicate powder showed low intensity and a broad diffraction peak at around $2\theta = 6.35°$ (corresponding to a d-spacing value of 1.38 nm).[14] Apart from this inter-atomic space between the two nanosilicate sheets, the XRD pattern of Laponite® RD from BYK additives shows crystalline peaks at $2\theta = 19.6°$, 34.8°, and 60.8°, in accordance with previous publications. Moreover, the XRD pattern of nanocellulose exhibited XRD peaks at $2\theta = 15^{o}$, 20.3^{o}, and 22.2^{o}, corresponding to the $(1\bar{1}0)$, (110), and (200) planes, respectively, which are characteristic cellulose I peaks.[28-29] Similar crystalline planes were also present in Lapolose along with the Laponite® RD-associated crystalline peak at $2\theta = 60.8°$; something that is in accordance with a successful nanosilicate incorporation into the paper films. The intensity of the $2\theta = 60.8°$ peak grew steadily as a function of nanosilicate content. Furthermore, the peak corresponding to the d-spacing at $2\theta = 6.35°$ completely disappeared in Lapolose due to the intercalation of nanocellulose and is, therefore, an indicator of successful exfoliation and dispersion of the nanosilicate in the

composites. Overall, the XRD results in Figure 2b fully support our assumption of a high nanosilicate exfoliation in the composites—an important facilitator of the speculated layer-by-layer Lapolose architecture (Figure 2a). From the XRD images, we were also able to determine the degree of crystallinity of Lapolose (Supporting Information Figure S1a). From here, it is evident that nanosilicate incorporation slightly increased the crystallinity index.

We used Fourier Transformation Infrared (FTIR) spectroscopy to further confirm successful incorporation of nanosilicate into nanocellulose paper (Supporting Information Figure S1b). Nanosilicate powder shows two major bands at 1040 and 680 cm^{-1}, assigned to Si-O-Si and Si-O stretching vibrations, respectively.[14] After nanosilicate incorporation, the Si-O-based stretching band at 1040 cm^{-1} shifts to 983 cm^{-1} due to hydrogen bond formation between nanosilicate and nanocellulose.[30] Additionally, Lapolose showed a new band at 650 cm^{-1} assigned to the deformation of Mg-O groups. Interestingly, the intensity of this band increased concomitantly with the degree of nanosilicate incorporation.

Cross-section scanning electron microscopy (SEM) of Lapolose with different nanoreinforcer concentrations is displayed in Figure 2c. The SEM images confirm the formation of the hypothesized nacre-mimetic structures. Additionally, chemical mapping performed through EDAX verified the presence of important mineral elements from nanosilicates such as magnesium and silica (Supporting Information Figure S2); while topographic atomic force microscopy (AFM) images show a negligible difference in the height contrast, suggesting that the Lapolose surface was homogeneous and smooth (Figure 2d). The root mean square (RMS) surface roughness for nanocellulose papers with nanosilicate concentration of 0%, 12%, 21% and 34% are 101.1±10.8 nm, 84.9±5.8 nm, 46.8±4.8 nm and 42.2±4.6 nm, respectively. In summary, the characterization studies in this section demonstrate that we could achieve well-dispersed incorporation of nanosilicate into Lapolose, which is critical for downstream electronic applications. The studies also prove

that these nanocellulose coated nanosilicates facilitated the formation of aligned and long-range lamellar structures in a similar vein as the hard phase of nacre.

Optical, thermal, barrier, mechanical, and stability properties of Lapolose

Figure 3a shows that the manufactured Lapolose is transparent in close proximity of an object and translucent when placed further away from it. Because the transparent substrates used in electronic devices typically are close to the source of electromagnetic radiation, we do not expect this optical effect to pose any challenges in display-based applications. As can be seen in Figure 3b, Lapolose could also easily fold and unfold—something that was not possible with the same ease for pristine NC. We examined these mechanical properties more in-depth through flexure analysis based on stress vs. strain measurements performed with a two-point-bending setup (Figure 3c). Our results show that both the ultimate flexural strength and modulus drop significantly after nanosilicate incorporation. This interesting trend has been quantified in a more detailed manner in Figure 3d, from which it can be concluded that both material flexural strength and modulus decreased almost four-fold from 28.9 ± 5.3 to 6.5 ± 1.4 MPa and from 6.0 ± 1.6 to 2.1 ± 0.5 GPa after 34% nanosilicate incorporation. A flexural modulus of 2.1 GPa is close to that of PET (1.5 to 2.8 GPa),[31-33] a petroleum-based polymer typically used as a substrate for flexible electronics.

In a similar vein, the tensile properties of Lapolose were quantified by using a conventional tensile testing setup (Figure 3e and 3f). We noted that nanosilicate incorporation up to 12% substantially increased both the tensile strength and the modulus from 69.4 ± 9.4 to 84.0 ± 15.5 MPa and from 3.7 ± 0.7 to 5.5 ± 1.1 GPa, respectively. Interestingly, the incorporation of nanosilicate brought the mechanical modulus within the range of that reported for traditional NC paper (6 – 30 GPa).[34-36] What's more, the incorporation of more than 12 % nanosilicate either did not result in additional reinforcement

or reduced it slightly (tensile strength). This was due to the suspension being too viscous and less exfoliated with some nanosilicate aggregates – something that all together compromised the formation of long-range nacre-mimetic like structures. These mechanical properties were further confirmed via AFM, since the Young's modulus of the Lapolose films with NS concentration of 34% was measured to be 6.02±1.83 GPa (Figure 3g).

Next, we characterized the chemical and thermal stability of Lapolose. Both of these are important for downstream applications involving device manufacturing and on-the-shelf performance. Here, the thermal stability of Lapolose was quantified by using thermal gravimetric analysis (TGA) (Figure 4a). From Figure 4a, it is evident that lesser mass loss occurred at high temperatures with Lapolose as compared to pristine nanocellulose. The onset temperature of thermal decomposition was increased from 290°C to 311°C after 34% nanosilicate incorporation (Figure 4b). In comparison, the thermal stability of PET and traditional NC substrates ranged between 400 and 450°C and between 250 and 300°C, respectively.[20, 37-39] Likewise, the dimensional stability of Lapolose in response to an increasing temperature rose substantially as a function of nanosilicate content, as was evident from the decrease in the coefficient of thermal expansion (CTE) (Figure 4c). Notably, this decrease went from a regime corresponding to that of conventional petroleum-based polymers (50-200 ppm/K)[19] and neared that of metals (10-25 ppm/K).[40] We note that the CTE value of our pristine NC was substantially higher than those reported in the literature for other NC variants (2 – 25 pmm/K).[9, 19] However, through nanosilicate incorporation, we could compensate for this shortcoming of AVAP® NC. Unlike the thermal properties of Lapolose, its chemical stability was unaffected by nanosilicate incorporation. In fact, pristine nanocellulose experienced almost no mass loss as the pH-value changed from 2 to 13 (Figure 4 d-f) or when in contact with different solvents (Supporting Information Figure S3).

Another important requirement of substrates used in electronic devices is a high

water-barrier as well as high surface hydrophilicity. In combination the two properties enable a stable device performance that is unaffected by various weatherly circumstances such as high humidity and extreme rainfall. Moreover; a low wettability is required for electronic substrates to facilitate easy substrate handling during the manufacturing process [3]. Therefore, we characterized the wettability of Lapolose at different points in time (Figure 4g). To that end, we noted that the wettability of all tested Lapolose variants was similar to current requirements in the field (60-80°).[9-10] Moreover, from the results in Figure 4g, it is evident that the contact angle was more stable with increasing nanosilicate content—something that could be due to the better water-barrier properties caused by the speculated nacre-mimetic architecture (Figure 2). Additionally, the water barrier properties of Lapolose were characterized by water permeation studies, where Lapolose was used as a filter membrane and 50 mL of water was allowed to pass through the paper. Interestingly, the nanosilicate-incorporated paper exhibited better water barrier due to its low water uptake properties (Figure 4g and Supporting Information Figure S4). Overall, the results displayed in Figure 4g confirm a nanosilicate-driven enhancement of barrier-properties and, thus, add an extra dimension to an already-broad material property portfolio. Barrier properties like those reported here are in contrast to traditional paper-based substrates, which tend to swell, lose mechanical integrity, and disintegrate in watery environments.[3, 41]

A Fleco wallpaper with electronic properties

The scope of this work is not merely to present a new material that could potentially replace conventional petroleum-based plastics. Rather, it is also to develop that could change the fundamentals of house building and flexible electronics. Particularly, in this section, we propose a new and exciting application for Lapolose—namely, a smart and electroactive wallpaper with radiant-like properties. In brief, this concept is about making large rolls of wallpaper, with incorporated electronic circuitry, that are easy to transport and that can

readily conform to walls or floors. This incorporated circuitry has three functions: A) an aesthetic function, by serving as a substitute for the wiring on small consumption electronics, such as clocks and small-sized speakers, via small and less-visible power lines; B) a "smart" function, by providing power, grounding, and data lines to "smart-home" sensors; and C) a "radiant" function, by providing prompt heat in the housing via the Joule effect.

To turn Lapolose into electronic wallpaper, electrodes were deposited on Lapolose in different patterns through a combination of E-beam evaporation and shadow masking (Figure 5a). Figure 5b shows foldable Lapolose with different gold circuits exhibiting geometries with a resolution of a few hundred microns. Interestingly, the metal patterns did not compromise the mechanical integrity of Lapolose and it retained its flexibility and foldability (Figure 5c). In this direction, we noticed that the electrical conductivity remained unchanged when Laplose was folded up to four numbers and bended for up to 150 ^{o} hundred times. This is an important requirement for flexible electronics such as the proposed smart wallpaper; as they need to be transported in a folded form and conform to various curved surfaces without losing their inherent electrical properties.

We later made an attempt towards manufacturing a green electronic paper capable of radiating heat by depositing a resistive serpentine gold pattern onto Lapolose. Figure 5d shows that by increasing the voltage with only 15 volt (V) the developed electronic paper can radiate substantial amount of heat through the electrical resistance meet during current flow inside a resistor. The principle here is known as "Joule heating". In Figure 5e, we quantified this heat generation and found that it is almost linearly proportional to the increase in volts. The slope of this linearity was 3.5°C/V from to 0 V to 15 V, amounting to a total temperature increase of 70°C. Heat generation in this range meets today's housing requirements; however, most importantly, we have shown that the generated heat could be obtained through small currents. Therefore, the exciting technology proposed herein requires

essentially very low power (>0.7 W) consumption (Supporting Information Figure S5). For this reason, the carbon footprint remains low at this end of the application chain as well.

Fleco-like 3D integrated electronics

Optically transparent substrates that are both Fleco-friendly and foldable while displaying the capacity to work in flexed and folded configurations can create a number of new avenues in the field of electronics. The wide range of applications of such electronic devices goes beyond flexible displays for portable computers, electronic wallpaper for smart housing, and wearable consumer electronics. Indeed, electronics that can roll into compact devices can yield a host of "out-of-box" scenarios for the electronics industry. Not only can this "so-called" rollable electronics (Rotronics) concept facilitate more efficient usage of space in electronic devices but it can also change the face of the computer processing industry. Indeed, the continuous race towards developing smaller, faster, bigger, better, and more compact consumer electronics has given rise to super-compact three-dimensional integrated circuits (3D-ICs) [42]. In this regard, the 3D-IC provides a route to achieve a significantly large memory cell density within a much smaller spatial area. Unfortunately, the substrates in most of these devices are silicon-based and the devices themselves consist of rigidly stacked processor circuits connected by even more rigid columnar conductors (Figure 6a). Obviously, this concept has its share of drawbacks including inefficient packing, bulkiness, low scalability, high cost, and inflexibility (Figure 6a). The working hypothesis in this section is that electronic Lapolose paper could potentially by origami-folding result in more appealing, efficient, and scalable 3D-ICs than the conventional ones.

More specifically, our hypothesis in this direction is that by simply depositing complex electronic circuitries on Fleco materials such as Lapolose, it is possible to build electronics that could roll into cable-like architectures consisting of 3D-ICs, where each circuit layer has been designed in a way such that it yields a global architecture specific to

the application at hand when over layered with adjacent circuits on the paper. This principle has been proof-of-concept demonstrated in Figure 6b-c, as we have shown that we can layer (squares, circles, and triangles) in predetermined architectures by depositing each of the circuit types in specific locations on Lapolose and then doing origami paper folding. Imagine, for a brief moment, that the circuit geometries in Figure 6b each correspond to specific component types such as nanometer-sized diodes and transistors. What would prevent the design proposition in Figure 6b from becoming a groundbreaking, functional, and real one in the industry? The electrical connections between the components, certainly. To that end, we have already demonstrated that the conductivity across the overlapping layers remained unchanged up to several paper folds. Furthermore, in Figure 6c, we demonstrate that Lapolose can be folded up to five times without it breaking, while in Figure 6d, we have carried out 3D tomography imaging of this and shown that we could layer the different component types in specific 3D locations.

Finally, in Figure 6e, we brought the concept of rotronics a bit closer to real-world applications by making a 3D-IC for "Joule heating". Notably, we folded the gold-based Lapolose resistor in Figure 5d into a folded wire-like structure (five folds) and exposed it to a DC voltage increase from 0 V to 3 V (Figure 6e). This small increase was sufficient to heat our rotronic heater to almost 30°. The 3D heating was evident through IR imaging; and the resultant 3D heat map is shown in Figure 6e. Specifically, the heat increase was linear, with a slope of 8 °C/V. Thus, we have given a simple "proof-of-concept demo" of the hidden potential of Fleco electronics as replacers of conventional and bulky 3D-IC-based consumer products.

Recycling

Here, we will close the recycling loop presented in Figure 1 by demonstrating that rotronic devices made from Lapolose are fully recyclable. In this direction, we use a simple, low-

cost, and eco-friendly procedure to remove the gold-based electronic circuits from Lapolose through a gentle treatment with HCL, followed by a brief sonication treatment (Figure 7a). Next, the paper was shredded mechanically with a shredder and subsequently mixed thoroughly with water to yield a gel-like substance characteristic of virgin nanocellulose. Notably, the re-dispersed Lapolose could easily be recast into new and functional paper films (Figure 7b). Indeed, the recycled Lapolose remained transparent and flexible, with mechanical properties that, within the calculated standard deviations, were fairly similar to those of the pristine ones, even after two recycling cycles. Likewise, we found that the contact angle and low CTE coefficient of the recycled Lapolose were similar to those of the pristine samples (Figure 7c). We, therefore, anticipate that the proposed Lapolose paper can give rise to electronics that have the capacity to facilitate better waste management in the industry while being compatible with high processing temperatures (up to 350°C) and substrate handlings (contact angle 75°) typically used in the manufacturing of conventional electronics.

Finally, we have demonstrated that the precious gold components of the Lapolose-based rotronics could easily be retrieved through exposure to heat, as Lapolose burned away rather quickly, while leaving the gold intact and ready to recycle from the leftover ashes (Figure 7d). This procedure would be a "no-go" with electronic substrates made from glass or metal, or from plastic substrates, for that matter. In addition, the burning of certain plastics can give rise to acute health problems due to the high emission of various toxins.[9, 43] In summary, it has been demonstrated that Lapolose-based electronics can easily be recycled into new devices using low-energy procedures with almost no CO_2 footprint. They are, therefore, ideal materials to use for the manufacture of sustainable and Fleco electronics and could help humanity prevent the impending e-waste disaster.

Discussion

Over the past years, an increasing trend towards paper electronics has arisen—a trend fueled by the work of George Whitesides and co-workers in 2007.[44-45] However, beyond its flexibility, paper does not exhibit any advantages over traditional materials used in electronics; indeed, it has its own share of drawbacks.[46] These include weak mechanical properties, rapid thermal degradation, and low stability in various demanding environments. NC-based paper, on the other hand, does not display these limitations. Unfortunately, the price of conventional nanopaper is substantially more than the price of ordinary paper. Therefore, the interest in using NC in electronics is still limited, as is evident from the low publication record in this area; in 2015, only 11 papers out of 1,000 NC-based publications detailed electronics.[19] Here, we have tried to address this gap in the field by using NC generated through a scalable and low-cost methodology in combination with nanosilicate reinforcement. Specifically, we have used it to develop electronic wallpaper for smart housing as well as a new methodology for replacing today's rigid 3D-ICs with less bulky ones.

Advantageously, we have demonstrated that proof-of-concept electronics deposited on our Lapolose could readily become rolled into compact and flexible 3D-IC's. Engineers began working on such circuits almost 20 years ago with limited success.[47] Indeed, the original concept entailed that the individual layers were made in parallel and then stacked and wired together through vertical silicon-based connections.[48] This scheme obviously increases the production time and, therefore, reduces the scalability of the technology. Another limitation with respect to the traditional view of 3D-ICs is related to the low vertical connector density in the devices, which, in turn, significantly compromises the flow of electricity between adjacent layers and the total data transfer volume.[42, 49] Though the so-called "monolithic integration methodology" (in which additional circuits are deposited onto the previous ones) enables 1,000 times more connector density, these integrated architectures

still have their fair share of drawbacks in terms of flexibility, production costs, and packing density.[50-51] Here, we have set forth some general guidelines in the field for addressing the abovementioned challenges through a simple and conventional lithographic device-manufacturing scheme onto rollable Lapolose-based paper. To that end, we have demonstrated that the resistance remains the same for the manufactured rotronic devices during flexing with a slight increase at around 5% after being bent to 150° and 20% after consecutive folds. Notably, we have shown that it is possible to manufacture a wire-like Joule heater by rolling a resistive gold-based circuit that, in its folded state, can function in a similar manner as it does in its unfolded state (Figure 6e). We do acknowledge that this is a very rough demonstration of an aspiring field; however, this manuscript is about a potentially groundbreaking concept within the field of electronics and is not intended to reveal all its beauty in the first attempt.

Amazingly, we have accomplished many of the abovementioned goals by simply mixing nanosilicate with "easy-to-upscale" and "cheaper-than-usual" AVAP® NC. From there, we generated ultra-thin Lapolose paper films. Indeed, through nanosilicate reinforcement, we were able to turn otherwise-inflexible AVAP® NC into flexible and foldable substrates. Arguably, the production of AVAP® NC is easier to scale up and is more environmentally friendly than those production methods based on mechanical treatment (grinding, shredding, and homogenization) of cellulose (high energy consumption) or multistep chemical processes involving sulfuric acid, sodium hydroxide, and household Clorox (high cost, slow production, non-environmentally friendly, and high energy consumption).[20-21] This is due in part to the use of more gentle solvents and chemicals such as sulfur dioxide and ethanol—and their subsequent recycling into the synthesis chain—during the process of removing hemicellulose, lignin, and amorphous cellulose. Interestingly, the AVAP® methodology also burns lignin from the NC precursor biomass to

generate power for the entire synthesis process, thereby, substantially lowers the net energy consumption. Another advantage of the process is the high NC crystallinity that it can yield—nearing almost 90%, and therefore one of the reasons why casted AVAP® NC paper was more inflexible than conventional counterparts in accordance with previous publications that compared highly crystalline NC with lesser crystalline counterparts.[52-53] In this regard, the nanosilicate incorporation could potentially disrupt the ordered fiber assembly and, in turn, make them easier to bend and flex. For instance, the positively charged edges of the nanosilicate could compete with the hydrogen bonding between adjacent NC fibers to facilitate more structure disorder.[30]

The state-of-the-art substrate for most flexible electronic devices is based on petroleum-based plastics such as PET and PEN.[54] This is due in part to the many exciting properties of plastic including flexibility, rollability, cost-efficiency, durability, and low weight. However, plastic does not degrade easily and, therefore, accumulates into piles of dangerous waste. These days, plastic also occupies a significant amount of land, while almost eight million metric tons of indestructible plastic debris reaches our oceans every year—a number that is expected to double by the end of 2025.[10] We, therefore, examined whether Lapolose-based electronics can be recycled without altering their original properties (Figure 7). In this direction, it was demonstrated that the metallic electrode part of the device could easily be removed. Notably, our results show that the underlying substrate could be recycled two times without compromising its mechanical, thermal, and wettability properties through low-energy processes at room temperature. In a similar vein, we have also shown that we could separate the precious metallic parts from the device through a simple burning procedure. This is in contrast to plastic, which, instead of turning into ash, melts into the embedded electronic—almost in a glue-like manner—while emitting potentially toxic

fumes.[43, 55] Overall, these results add an extra dimension to an already impressive range of "can-do's".

Another exciting quality of the technology proposed in this paper is related to its scalability and low cost. Indeed, the cost of Lapolose per square decimeter is $0.016 and the cost of manufacturing the rotronic heaters is less than $1. By contrast, PET-based substrates cost approximately $0.02 per dm^{-2}, while their more expensive counterpart, polyimide, costs $0.30 per dm^{-2}.[56] Additionally, the thermal stability of most plastics, with PI being an exception, is mostly below 300°C [57] and, thus, they cannot endure the high processing temperatures used during the manufacturing of transistors and semiconductors (up to 350°C).[58] The cost-effectiveness and Fleconesss also enable Lapolose-based electronics to become mass-producible without inflicting any threats on the environment. For the same reason, the futuristic paper developed herein is applicable for applications that require large surface areas such as displays for computers, television sets, mobile phones, billboards, electronic wallpaper, and various industrial machines.

Conclusions

Nanocellulose (NC) has emerged as a material that, due to its low weight, excellent mechanical properties, high thermal stability, and sustainability, can potentially replace a number of non-renewable, high-cost, and non-sustainable materials, including petroleum-based polymers and precious metals, as well as more abundant and frequently used ones such as steel and glass. Unfortunately, one of the obstacles in this regard is the low NC scalability. Here, we have addressed these issues by combining nanosilicate with AVAC NC to yield a substrate with the same remarkable properties as traditional NC but at a cost-competitive price comparable to that of plastics. In a demonstration study, we deposited a resistive-gold-based pattern onto Lapolose to generate a heat sensor and showed that it could function in a 3D-IC state without compromising the electrical connections. Additionally, we

showed that different complex circuitries could be over-layered, one over another, to yield a 3D-IC with only a 20% drop in electrical flow between the bottom- and top-most layers. We have therefore unlocked the first door to the realm of paper-based 3D-ICs. The authors envision that further progress in this direction will inevitably lead to many exciting applications in which sensors, CPUs, memory devices, and resistors are combined into compact and sophisticated electronics. Indeed, such futuristic components could herald a new era for soft robotics, cyborganics, smart biorobots, and artificial cyborg-like creatures, as the keys to this application portfolio are compact, flexible, and versatile electronic circuits.

Materials and Methods

Preparation of Laponite® reinforced Nanocellulose (Lapolose) paper

Nacre-mimetic Lapolose paper was prepared by hot pressing the mixture suspension containing nanocellulose fibrils and nanosilicates. In brief, 240 g of 2.4 wt% nanocellulose fibrils suspension (NC, AVAP® technology, American Process) were mixed with different amounts of nanosilicates (Laponite® RD, BYK additives, UK) in order to get different compositions (0%, 12%, 21% and 34%). The required amount of nanosilicates were separately dispersed in 150 mL of Milli-Q (MQ) water by stirring for 2 hours and slowly mixed with NC suspension by blending 8 times with high-speed blender (Philips Problender 6). The resulted suspension were allowed to stand at room temperature for 24 hours in order to react the NC and nanosilicates and blended again 8 times with blender. To make the paper, approximately 40g of the suspensions were sandwiched between two stainless steel (150 mesh wire cloth woven) sheets (10 x 10 cm) and hot pressed at 60 ^{o}C on a hotplate under a pressure of 100N (10 kg) for 2 days. For making paper by casting method, 15 g of thick suspensions were diluted to 30 mL with MQ water and sonicated for 1 hour. The mixture solutions were casted onto a petri dish and dried on a hot plate at 60 ^{o}C for 24 hours.

X-ray powder diffraction (XRD) analysis

XRD analysis of Lapolose paper were performed at room temperature with a HUBER G670 (Guinier geometry with imaging-plate detector) X-ray powder diffractometer (Germany) with Cu Kα1 monochromatic radiation (λ = 1.54056 Å) equipped with a Ge(111) monochromator, which operates at 40 kV and 40 mA. XRD patterns were collected with 2θ ranging from 3° to 80° and a scan step size of 0.005°. The crystallinity index of the Lapolose paper were calculated from the maximum intensity of the crystalline peak (I_{200}) at 2θ= 22.2° and amorphous region (I_{am}) at 2θ= 18.6° using the following equation [59].

$$\text{Crystallinity index (\%)} = \frac{I_{200} - I_{am}}{I_{200}} \times 100 \quad (1)$$

Scanning electron microscopy (SEM) and energy-dispersive X-ray spectroscopy (EDX) analysis

The cross-sectional images of the Lapolose paper were observed by a FEI Quanta 200 ESEM FEG Scanning Electron Microscope (USA) operating at 10 kV and 10 mA. In order to get the uniform cross-section, the paper samples were broken after immersing in liquid nitrogen and mounted on a 45° SEM stub. Prior to the SEM imaging, all the samples were sputter-coated with 10 nm gold. An Oxford Instruments X-Max silicon drift detector (UK) connected to the SEM instrument with an 80 mm^2 detection area was used to perform the EDX characterization of the paper. All EDX measurements were carried out before gold sputtering. .

Atomic force microscopy (AFM) imaging

AFM characterizations were performed at a Cypher ES AFM (Asylum Research, USA) at ambient conditions using AM-FM mode. Silicon cantilevers (OMCL-AC160TS-R3;

Olympus) with a nominal spring constant of 26 N m^{-1} were employed. The Young's modulus was fitted using the Sneddon model.

Fourier-Transform Infrared (FTIR) analysis

Attenuated total reflectance (ATR)-FTIR spectra of the Lapolose paper were collected using a PerkinElmer Spectrum 100 FTIR spectrometer (USA). The sampleas were scanned at a resolution of 4 cm^{-1} with 16 scans in the range of 4000 - 500 cm^{-1} at 25 ºC. Subsequently, the baseline of the spectra were corrected and normalized using PerkinElmer Spectrum software.

Thermal properties

Thermal stability of Lapolose was measured using a TA instruments TGA Q500 Thermogravimetric analyzer (USA). Thermogravimetric analysis (TGA) was conducted in a nitrogen atmosphere (60 mL min^{-1}) by heating the various samples from 30 to 900 ºC at a rate of 10 ºC min^{-1}. A rheometric solid analyzer was used to find out the coefficient of thermal expansion (CTE). A dynamic temperature ramp test was performed on 50 mm × 5 mm under nitrogen atmosphere from 25 to 75 ºC at a heating rate of 5 ºC min^{-1}. The measurements were performed at constant strain of 1.0% by applying a constant force of 0.03N in tensile mode and a frequency of 1.0 Hz. The slope of the linear expansion (ΔL/L) -temperature curve were determined and reported as CTE values [14].

Moisture uptake studies

The moisture uptake of the Lapolose paper was determined at different humidity conditions. The paper was stored at relative humidity 10 and 90 and the weighed before (W_o) and after 24 hours (W_u) using a precision analytical balance and the moisture content (%) of the films were calculated using the following equation:

$$\text{Moisture Content (\%)} = \frac{W_o - W_u}{W_o} \times 100 \quad (2)$$

Chemical stability

The stability of Lapolose papers was assessed in different pH solutions from 2.0-13.0 and in various organic solvents such as acetone, ethanol and toluene. The lapolose papers were immersed in corresponding solutions at room temperature and dried at 60 ^{o}C. Initial weight (W_o) and dry weight at each time point (W_t) of the films were recorded. The following equation were used to calculate weight loss after after each time points:

$$\text{Weight (\%)} = \frac{W_o - W_t}{W_o} \times 100 \quad (3)$$

Water contact angle study

The static water contact angle of the Lapolose paper was measured using a Biolin Scientific Holding AB Attension Theta optical tensiometer (Sweden) equipped with a high-speed camera. The contact angle were determined by fitting droplet shapes by the Young-Laplace method using Attention theta software. . In order to the static contact angle change over time, water droplets of 10 µl were deposited on the lapolose films surface, and the contact angle estimated at different time intervals up to 600 s.

Mechanical properties

Mechanical properties of Lapolose were performed with an Instron 5967 Universal Testing Systems (UK). For tensile measurements, the lapolose paper were cut into a rectangular shape of 30 mm length and 2 mm width using an Epilog laser-cutting machine and the guage length were set to 10 mm. The thickness of the paper films was varied from 40 to 90 µm, which was measured using a digital electronic Vernier caliper before the test. Tests were conducted using a 500 N load-cell by straining at a rate of 1 mm min^{-1} until the failure point was reached. The stress−strain curve was recorded using Bluehill 3 testing software. For

three-point bending tests, samples of 60 mm length and 17 mm were tested using a loading velocity of 15 mm/min and a span length of 30 mm.

Patterned electrode deposition on Lapolose

Shadow mask technique: The deposition of gold on Lapolose were achieved in two steps using shadow mask lithography. In the first step, a shadow mask was designed on 525 ± 25 µm silicon wafer using photolithography. Shortly after, the silicon wafer was spin coated with 4µm photoresist (AZ MiR 701) and a pre-determined pattern was created through a photomask. In the second step, electron beam evaporation technique was used to deposit metals on Lapolose. Here, the moisture from Lapolose were removed through heating at 90 ^{o}C for 10 minutes on a hot plate and securely placed under the shadow mask. Chromium layer of 50 nm with a rate of 5 Å/s at the bottom and a Gold (Au) layer of 150 nm with a rate of 10 Å/s on the top was deposited onto Lapolose through the shadow mask using a Physimeca electron beam evaporation system (Physimeca Technologies, France). Various resistive serpentine patterns were printed on Lapolose and examined through the optical microscope. For making patterns with silver paste, the patterns were created on a 500 µm polyester film using laser cutting (Epilog Mini24 CO_2 laser) and securely placed on top of Lapolose. The silver epoxy paste was coated with a blade on the polymer films, and then carefully removed from Lapolose, and dried at room temperature for 24 hours to create a silver electrode patterns on Lapolose.

Resistance measurements

The resistances of the metal patterned electrodes were examined at room temperature using the 2-wire method with a digital multimeter (fluke-45-dual-display-multimeter). The initial resistance of the patterned gold and silver were 80±10 Ω and 15±5 Ω, respectively. The ratio of the initial resistance (Ro) and the resistance after bending or folding (R) is reported.

Joule heater fabrication and measurements

Gold or silver printed resistors on Lapolose was used for the fabrication of the joule heater. To fabricate a heater, both ends of metal patterns were connected with copper wires using silver epoxy paste. These copper wires were connected to a RIGOL DP832A programmable DC power supply to apply voltage to the resistors. Voltage was increased stepwise using constant current mode and the heat released due to the increased voltage was monitored using FLIR T650sc portable thermal imaging camera. The average temperature around the electrode area *vs* voltage is reported.

Rollable electronics (Rotronics) fabrication and characterization

The printed resistors were connected with copper wires using silver epoxy paste and carefully rolled to fabricate the rotronics. The resistance of the rotronics were measured with a digital multimeter and the rolling of the Lapolose electrodes were visualized using a confocal laser scanning microscope (CLSM, Zeiss LSM 700, Germany). X-ray computed tomography (CT) images of the rotronics was acquired using ZEISS Xradia 410 Versa submicron X-ray imaging systems with a resolution of 1–50 μm in samples of size 1–50 mm. The thermal measurements on the rotronics were performed as described previously.

Recycling of Lapolose

Initially, the gold layer from Lapolose was removed by sonicating for 2 minutes using 1M HCl. To recycle the Lapolose, the dried paper films were shredded into powder using a high-speed blender (Philips Problender 6). The required amount of MQ water was added to make the NC suspension and blended continuously for 2-3 hours. The blended suspension of recycled paper was casted on a petri dish at 60 ^{o}C for 24 hours. Mechanical properties and contact angle of the recycled films were measured as described in the previous section. For

the combustion experiments, the electrode printed Lapolose films were ignited using a commercial lighter and burned until it turned into.

Acknowledgements

ADP would like to acknowledge the Danish Council for Independent Research (Technology and Production Sciences, 8105–00003B), the Villum Foundation (10103) and the VIDI research programme with project number R0004387, which is (partly) financed by the Netherlands Organisation for Scientific Research (NWO). MA thanks the Canadian Institutes for Health Research (CIHR) for supporting this work. The authors would also like to thank DTU Nanolab for support in cleanroom facilities to deposit gold pattern using lithographic techniques.

Supporting Information

Crystallinity calculated from XRD; brief description and FTIR analysis of the Lapolose films; cross-sectional SEM-EDX spectra of Lapolose films with NS concentration varying from 0 to 34 wt%; chemical stability of NC-LRD composites in Acetone, Ethanol and Toluene at different relative humidity (RH) values; weight gained at RH 90 and weight loss at RH 10 of the Lapolose films; and power of the joule heater with respect to voltage."

References

(1) Geyer, R.; Blass, V. D. The Economics of Cell Phone Reuse and Recycling. *Int. J. Adv. Manuf. Tech.* **2010,** *47*, 515-525.

(2) Robinson, B. H. E-waste: An Assessment of Global Production and Environmental Impacts. *Sci. Total Environ.* **2009,** *408*, 183-191.

(3) Jung, Y. H.; Chang, T.-H.; Zhang, H.; Yao, C.; Zheng, Q.; Yang, V. W.; Mi, H.; Kim, M.; Cho, S. J.; Park, D.-W. High-Performance Green Flexible Electronics Based on Biodegradable Cellulose Nanofibril Paper. *Nat. commun.* **2015,** *6*, 7170.

(4) Han, T.-H.; Kim, H.; Kwon, S.-J.; Lee, T.-W. Graphene-Based Flexible Electronic Devices. *Mater. Sci. Eng. R Rep.* **2017,** *118*, 1-43.

(5) Yun, Y. J.; Hong, W. G.; Choi, N.-J.; Kim, B. H.; Jun, Y.; Lee, H.-K. Ultrasensitive and Highly Selective Graphene-Based Single Yarn for Use in Wearable Gas Sensor. *Sci. Rep.* **2015,** *5*, 10904.

(6) Singh, E.; Meyyappan, M.; Nalwa, H. S. Flexible Graphene-Based Wearable Gas and Chemical Sensors. *ACS Appl. Mater. Interfaces* **2017,** *9*, 34544-34586.

(7) Liou, Y.-R.; Lin, H. Y.; Shen, T. L.; Cai, S. Y.; Wu, Y. H.; Liao, Y. M.; Lin, H. I.; Chen, T. P.; Lin, T. Y.; Chen, Y. F. Integration of Nanoscale and Macroscale Graphene Heterostructures for Flexible and Multilevel Nonvolatile Photoelectronic Memory. *ACS Appl. Nano Mater.* **2019,** *3*, 608-616.

(8) Choi, M.; Park, Y. J.; Sharma, B. K.; Bae, S.-R.; Kim, S. Y.; Ahn, J.-H. Flexible Active-Matrix Organic Light-Emitting Diode Display Enabled by MoS_2 Thin-Film Transistor. *Sci. Adv.* **2018,** *4*, eaas8721.

(9) Gao, L.; Chao, L.; Hou, M.; Liang, J.; Chen, Y.; Yu, H.-D.; Huang, W. Flexible, Transparent Nanocellulose Paper-Based Perovskite Solar Cells. *npj Flex. Electron.* **2019,** *3*, 4.

(10) Jiang, F.; Li, T.; Li, Y.; Zhang, Y.; Gong, A.; Dai, J.; Hitz, E.; Luo, W.; Hu, L. Wood‐Based Nanotechnologies toward Sustainability. *Adv. Mater.* **2018,** *30*, 1703453.

(11) Wei, R.; Zimmermann, W. Microbial Enzymes For The Recycling of Recalcitrant Petroleum‐Based Plastics: How Far are We? *Microb. Biotechnol.* **2017,** *10*, 1308-1322.

(12) Sun, H.-S.; Chiu, Y.-C.; Chen, W.-C. Renewable Polymeric Materials for Electronic Applications. *Polym. J.* **2017,** *49*, 61.

(13) Zhu, B.; Wang, H.; Leow, W. R.; Cai, Y.; Loh, X. J.; Han, M. Y.; Chen, X. Silk Fibroin for Flexible Electronic Devices. *Adv. Mater.* **2016,** *28*, 4250-4265.

(14) Kadumudi, F. B.; Jahanshahi, M.; Mehrali, M.; Zsurzsan, T. G.; Taebnia, N.; Hasany, M.; Mohanty, S.; Knott, A.; Godau, B.; Akbari, M. A Protein‐Based, Water‐Insoluble, and Bendable Polymer with Ionic Conductivity: A Roadmap for Flexible and Green Electronics. *Adv. Sci.* **2019,** *6*, 1801241.

(15) Moreno, S.; Baniasadi, M.; Mohammed, S.; Mejia, I.; Chen, Y.; Quevedo‐Lopez, M. A.; Kumar, N.; Dimitrijevich, S.; Minary‐Jolandan, M. Biocompatible Collagen Films as Substrates for Flexible Implantable Electronics. *Adv. Electron. Mater.* **2015,** *1*, 1500154.

(16) Nogi, M.; Iwamoto, S.; Nakagaito, A. N.; Yano, H. Optically Transparent Nanofiber Paper. *Adv. Mater.* **2009,** *21* (16), 1595-1598.

(17) Zhu, H.; Luo, W.; Ciesielski, P. N.; Fang, Z.; Zhu, J.; Henriksson, G.; Himmel, M. E.; Hu, L. Wood-Derived Materials for Green Electronics, Biological Devices, and Energy Applications. *Chem. Rev.* **2016,** *116*, 9305-9374.

(18) Zhu, M.; Song, J.; Li, T.; Gong, A.; Wang, Y.; Dai, J.; Yao, Y.; Luo, W.; Henderson, D.; Hu, L. Highly Anisotropic, Highly Transparent Wood Composites. *Adv. Mater.* **2016,** *28*, 5181-5187.

(19) Hoeng, F.; Denneulin, A.; Bras, J. Use of Nanocellulose in Printed Electronics: A Review. *Nanoscale* **2016,** *8*, 13131-13154.

(20) Nelson, K.; Retsina, T.; Iakovlev, M.; van Heiningen, A.; Deng, Y.; Shatkin, J. A.; Mulyadi, A. *American Process: Production of Low Cost Nanocellulose for Renewable, Advanced Materials Applications. In Materials Research for Manufacturing;* Springer, Cham, 2016; pp 267-302.

(21) Nelson, K.; Retsina, T. Innovative Nanocellulose Process Breaks the Cost Barrier. *TAPPI J* **2014,** *13*, 19-23.

(22) Palavesam, N.; Marin, S.; Hemmetzberger, D.; Landesberger, C.; Bock, K.; Kutter, C. Roll-To-Roll Processing of Film Substrates for Hybrid Integrated Flexible Electronics. *Flex. Print. Electron.* **2018,** *3*, 014002.

(23) Lee, B.-H.; Lee, D.-I.; Bae, H.; Seong, H.; Jeon, S.-B.; Seol, M.-L.; Han, J.-W.; Meyyappan, M.; Im, S.-G.; Choi, Y.-K. Foldable and Disposable Memory on Paper. *Sci. Rep.* **2016,** *6*, 1-8.

(24) Avery, R. K.; Albadawi, H.; Akbari, M.; Zhang, Y. S.; Duggan, M. J.; Sahani, D. V.; Olsen, B. D.; Khademhosseini, A.; Oklu, R. An Injectable Shear-Thinning Biomaterial for Endovascular Embolization. *Sci. Transl. Med.* **2016,** *8*, 365ra156-365ra156.

(25) Samimi Gharaie, S.; Dabiri, S.; Akbari, M. Smart Shear-Thinning Hydrogels as Injectable Drug Delivery Systems. *Polymers* **2018,** *10*, 1317.

(26) Hasany, M.; Thakur, A.; Taebnia, N.; Kadumudi, F. B.; Shahbazi, M.-A.; Pierchala, M. K.; Mohanty, S.; Orive, G.; Andresen, T. L.; Foldager, C. B. Combinatorial Screening of Nanoclay-Reinforced Hydrogels: A Glimpse of the "Holy Grail" in Orthopedic Stem Cell Therapy? *ACS Appl. Mater. Interfaces* **2018,** *10*, 34924-34941.

(27) Talebian, S.; Mehrali, M.; Taebnia, N.; Pennisi, C. P.; Kadumudi, F. B.; Foroughi, J.; Hasany, M.; Nikkhah, M.; Akbari, M.; Orive, G. Self‐Healing Hydrogels: The Next Paradigm Shift in Tissue Engineering? *Adv. Sci.* **2019,** *6*, 1801664.

(28) Peng, Y.; Gardner, D. J.; Han, Y.; Kiziltas, A.; Cai, Z.; Tshabalala, M. A. Influence of Drying Method on the Material Properties of Nanocellulose I: Thermostability and Crystallinity. *Cellulose* **2013,** *20*, 2379-2392.

(29) Chen, Y. W.; Lee, H. V. Revalorization of Selected Municipal Solid Wastes as New Precursors of "Green" Nanocellulose via a Novel One-Pot Isolation System: A Source Perspective. *Int. J. Biol. Macromol.* **2018,** *107*, 78-92.

(30) Zhou, S.; Wang, M.; Yang, J.; Xu, F. Structure and Mechanical Properties of Transparent Layered Nanocomposites from LAPONITE®-Hydroxyethyl Cellulose Vacuum-Assisted Self-Assembly. *RSC Adv.* **2015,** *5*, 35976-35984.

(31) Doğan, M.; Erdoğan, S.; Bayramlı, E. Mechanical, Thermal, and Fire Retardant Properties of Poly (Ethylene Terephthalate) Fiber Containing Zinc Phosphinate and Organo-Modified Clay. *J. Therm. Anal. Calorim.* **2013,** *112*, 871-876.

(32) Novello, M. V.; Carreira, L. G.; Canto, L. B. Post-Consumer Polyethylene Terephthalate and Polyamide 66 Blends and Corresponding Short Glass Fiber Reinforced Composites. *Mater. Res.* **2014,** *17*, 1285-1294.

(33) Ardekani, S. M.; Dehghani, A.; Al-Maadeed, M. A.; Wahit, M. U.; Hassan, A. Mechanical and Thermal Properties of Recycled Poly (Ethylene Terephthalate) Reinforced Newspaper Fiber Composites. *Fibers Polym.* **2014,** *15*, 1531-1538.

(34) Fang, Z.; Hou, G.; Chen, C.; Hu, L. Nanocellulose-Based Films and Their Emerging Applications. *Curr. Opin. Solid State Mater. Sci.* **2019,** *23*, 100764.

(35) Zhu, H.; Xiao, Z.; Liu, D.; Li, Y.; Weadock, N. J.; Fang, Z.; Huang, J.; Hu, L. Biodegradable Transparent Substrates for Flexible Organic-Light-Emitting Diodes. *Energy Environ. Sci.* **2013,** *6*, 2105-2111.

(36) Zhu, H.; Fang, Z.; Preston, C.; Li, Y.; Hu, L. Transparent Paper: Fabrications, Properties, and Device Applications. *Energy Environ. Sci.* **2014,** *7*, 269-287.

(37) Shah, J.; Jan, M. R. Effect of Polyethylene Terephthalate on the Catalytic Pyrolysis of Polystyrene: Investigation of the Liquid Products. *J. Taiwan Inst. Chem. Eng.* **2015,** *51*, 96-102.

(38) Wang, C. S.; Shieh, J. Y.; Sun, Y. M. Synthesis and Properties of Phosphorus Containing PET and PEN (I). *J. Appl. Polym.* **1998,** *70*, 1959-1964.

(39) Li, J.; Mooney, D. J. Designing Hydrogels for Controlled Drug Delivery. *Nat. Rev. Mater.* **2016,** *1* (12), 16071.

(40) Cverna, F. *ASM Ready Reference: Thermal Properties of Metals*, ASM International: 2002.

(41) Wang, J.; Gardner, D. J.; Stark, N. M.; Bousfield, D. W.; Tajvidi, M.; Cai, Z. Moisture and Oxygen Barrier Properties of Cellulose Nanomaterial-Based Films. *ACS Sustain. Chem. Eng.* **2017,** *6*, 49-70.

(42) Reda, S. Electronics: 3D Integration Advances Computing. *Nature* **2017,** *547*, 38.

(43) Verma, R.; Vinoda, K.; Papireddy, M.; Gowda, A. Toxic Pollutants from Plastic Waste-A Review. *Procedia Environ. Sci.* **2016,** *35*, 701-708.

(44) Martinez, A. W.; Phillips, S. T.; Butte, M. J.; Whitesides, G. M. Patterned Paper as a Platform for Inexpensive, Low‐Volume, Portable Bioassays. *Angew. Chem. Int.* **2007,** *46*, 1318-1320.

(45) Martinez, A. W.; Phillips, S. T.; Wiley, B. J.; Gupta, M.; Whitesides, G. M. FLASH: A Rapid Method For Prototyping Paper-Based Microfluidic Devices. *Lab Chip* **2008,** *8*, 2146-2150.

(46) Lin, Y.; Gritsenko, D.; Liu, Q.; Lu, X.; Xu, J. Recent Advancements in Functionalized Paper-Based Electronics. *ACS Appl. Mater. Interfaces* **2016,** *8*, 20501-20515.

(47) Tu, K. Reliability Challenges in 3D IC Packaging Technology. *Microelectron. Reliab.* **2011,** *51*, 517-523.

(48) Lau, J. H. Overview and Outlook of Through-Silicon Via (TSV) and 3D Integrations. *Microelectron. Int.* **2011,** *28*, 8-22.

(49) Shulaker, M. M.; Hills, G.; Park, R. S.; Howe, R. T.; Saraswat, K.; Wong, H.-S. P.; Mitra, S. Three-Dimensional Integration of Nanotechnologies for Computing and Data Storage on a Single Chip. *Nature* **2017,** *547*, 74.

(50) Burghartz, J. N.; Ferwana, S.; Harendt, C. *In Ultrathin Chips for Flexible Electronics and 3D ICs*, 2015 IEEE SOI-3D-Subthreshold Microelectronics Technology Unified Conference (S3S), IEEE: 2015; pp 1-3.

(51) Beica, R. In *3D Integration: Applications and Market Trends*, 2015 International 3D Systems Integration Conference (3DIC), IEEE: 2015; pp TS5. 1.1-TS5. 1.7.

(52) Petroudy, S. D. Physical And Mechanical Properties Of Natural Fibers. *In Advanced High Strength Natural Fibre Composites in Construction*; Elsevier: 2017; pp 59-83.

(53) Moon, R. J.; Martini, A.; Nairn, J.; Simonsen, J.; Youngblood, J. Cellulose Nanomaterials Review: Structure, Properties and Nanocomposites. *Chem. Soc. Rev.* **2011,** *40*, 3941-3994.

(54) MacDonald, W. A.; Looney, M.; MacKerron, D.; Eveson, R.; Adam, R.; Hashimoto, K.; Rakos, K. Latest Advances in Substrates for Flexible Electronics. *J. Soc. Inf. Disp.* **2007,** *15*, 1075-1083.

(55) Casasanta III, V., inventor; Empire Technology Development LLC, assignee. Biodegradable Printed Circuit Boards and Methods for Making the Printed Circuit Boards. *United States patent application* **2017**, US 15/125,573.

(56) Tobjörk, D.; Österbacka, R. Paper Electronics. *Adv. Mater.* **2011,** *23*, 1935-1961.

(57) McKeen, L. W. *Film Properties of Plastics and Elastomers*, William Andrew: 2017.

(58) Choi, M.-C.; Kim, Y.; Ha, C.-S. Polymers for Flexible Displays: From Material Selection to Device Applications. *Prog. Polym. Sci.* **2008,** *33*, 581-630.

(59) Trifol, J.; Sillard, C.; Plackett, D.; Szabo, P.; Bras, J.; Daugaard, A. E. Chemically Extracted Nanocellulose from Sisal Fibres by a Simple and Industrially Relevant Process. *Cellulose* **2017,** *24*, 107-118.

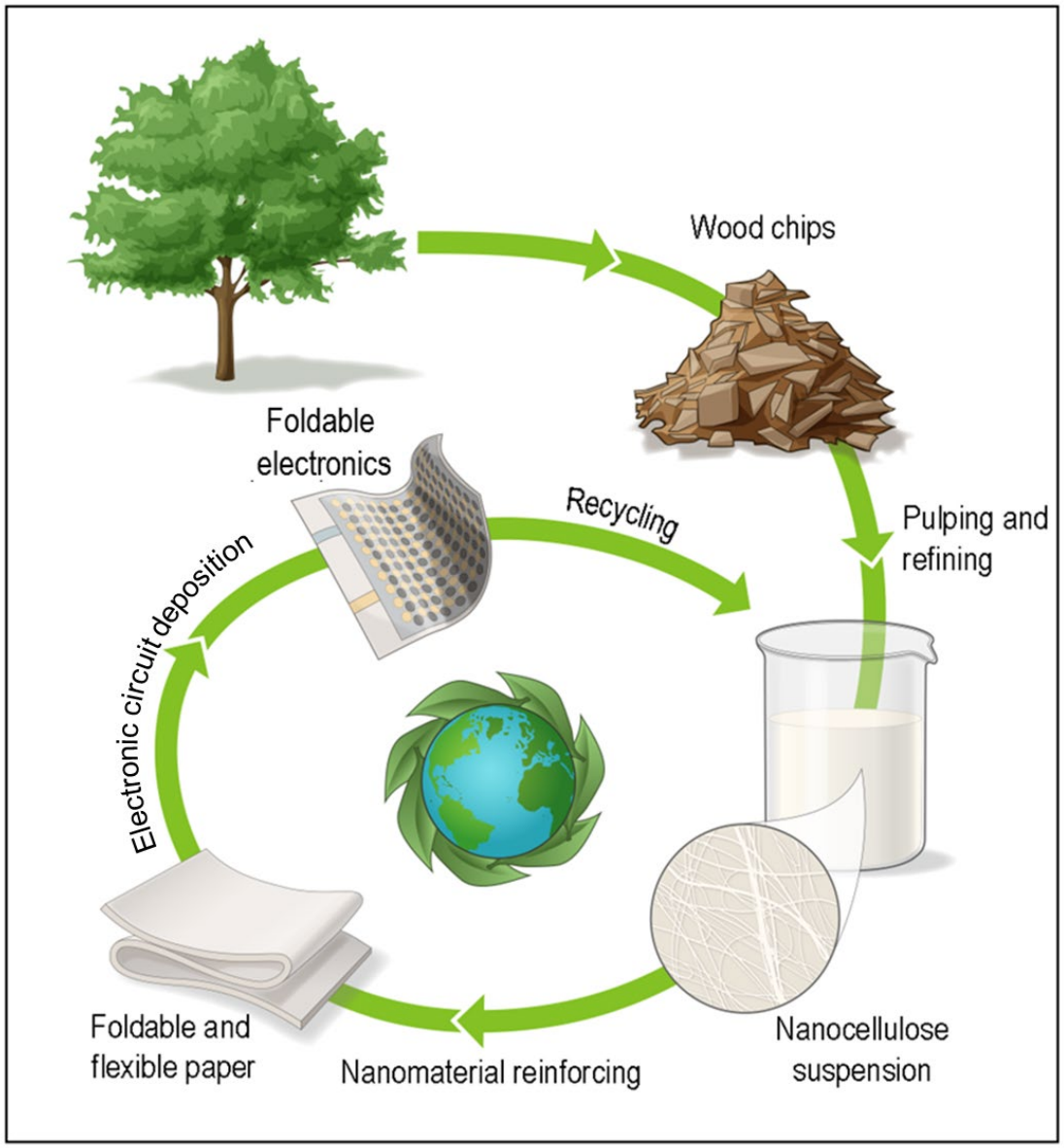

Figure 1. A green future based on foldable, flexible and recyclable wood-based electronics that can fold and roll into complex 3D integrated circuits.

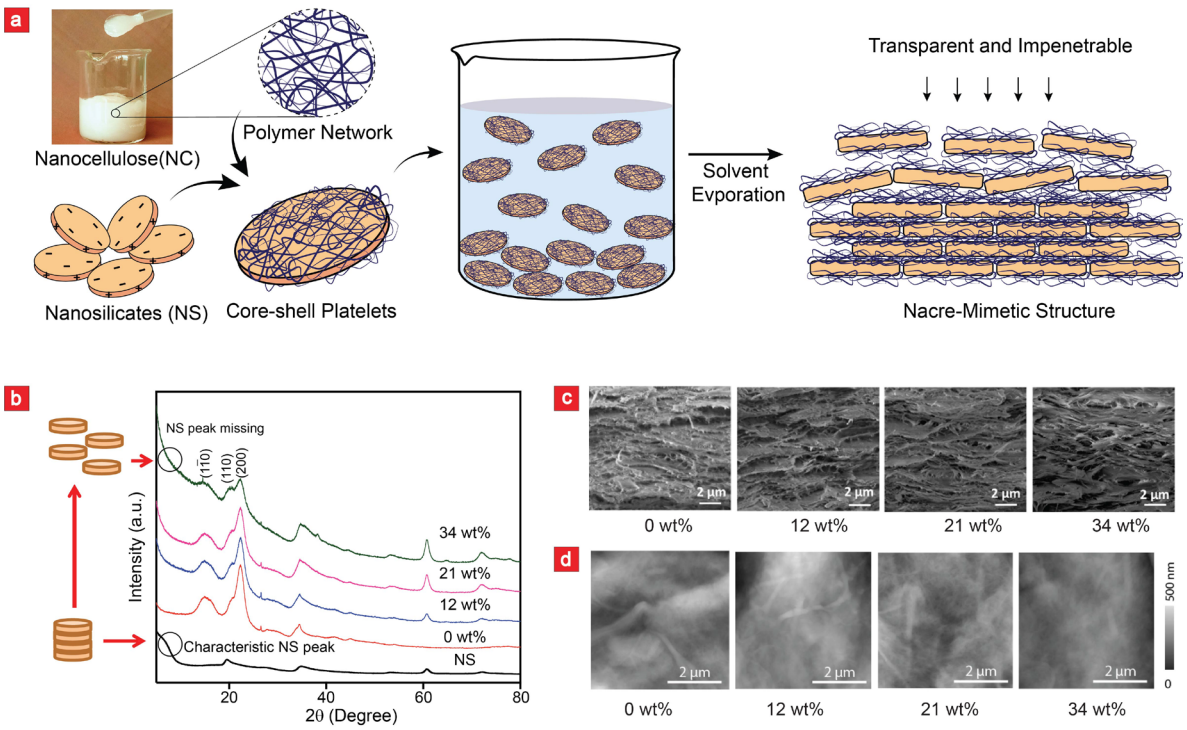

Figure 2. Preparation of Nanosilicate reinforced nanocellulose (Lapolose). **(a)** Self-assembled and brick-and-mortar-like Lapolose films generated through solution casting. **(b)** XRD characterization, **(c)** Cross-sectional Scanning Electron Microscopy (SEM) images and **(d)** AFM analysis of Lapolose films with NS concentration varying from 0 to 34 wt%.

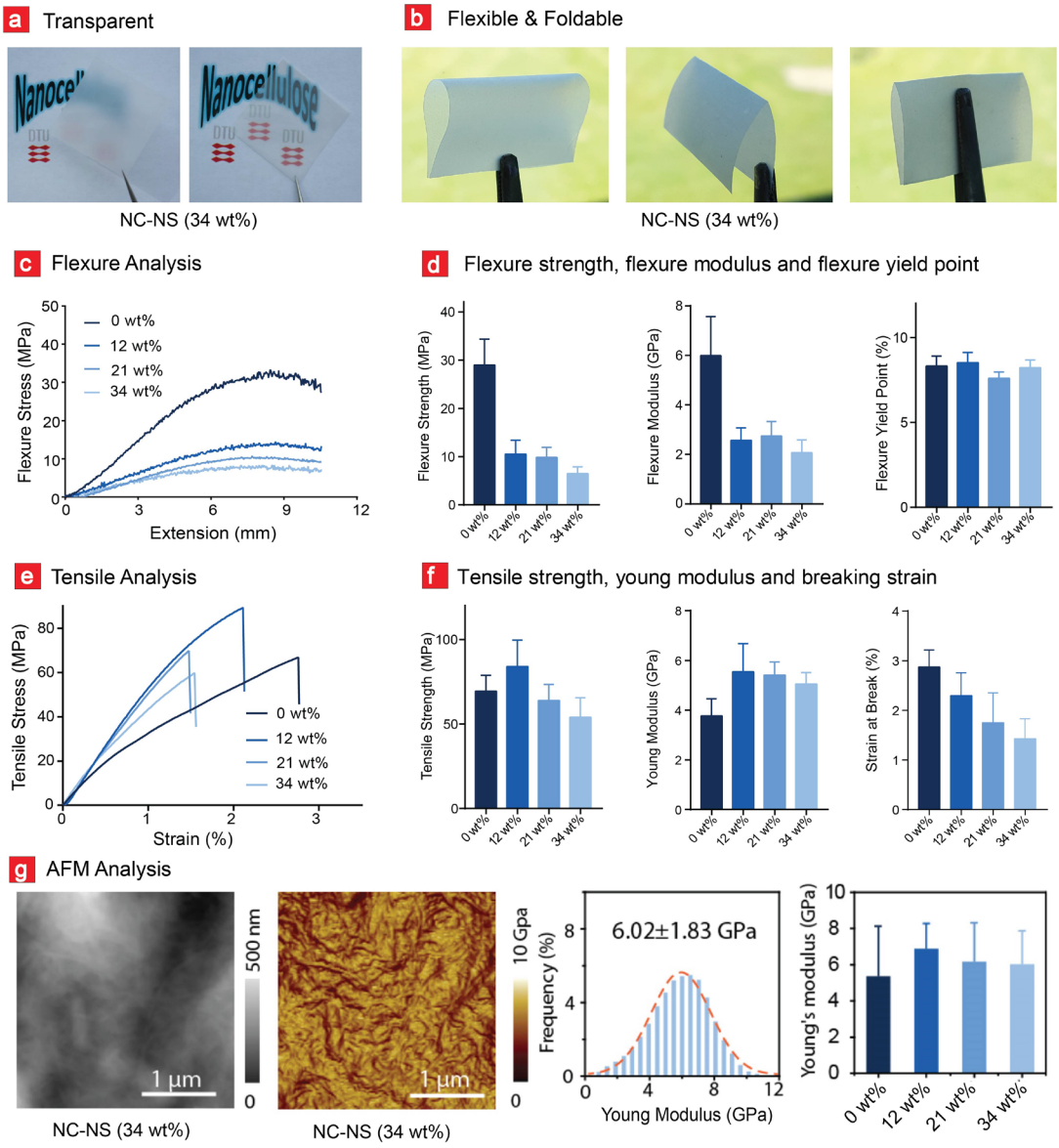

Figure 3. Optical and mechanical properties. Lapolose (34 wt%) was (a) optically transparent, (b) flexible and foldable. (c) Stress-strain curves corresponding to the performed flexure tests with an Instron mechanical tester and (d) the associated flexure strength, flexure modulus and flexure yield point. (e) Stress-strain curves corresponding to the performed tensile test. (f) The tensile strength, young modulus and breaking strain were retrieved from the stress strain curved and displayed here. (g) AFM mechanical analysis and corresponding young's modulus..

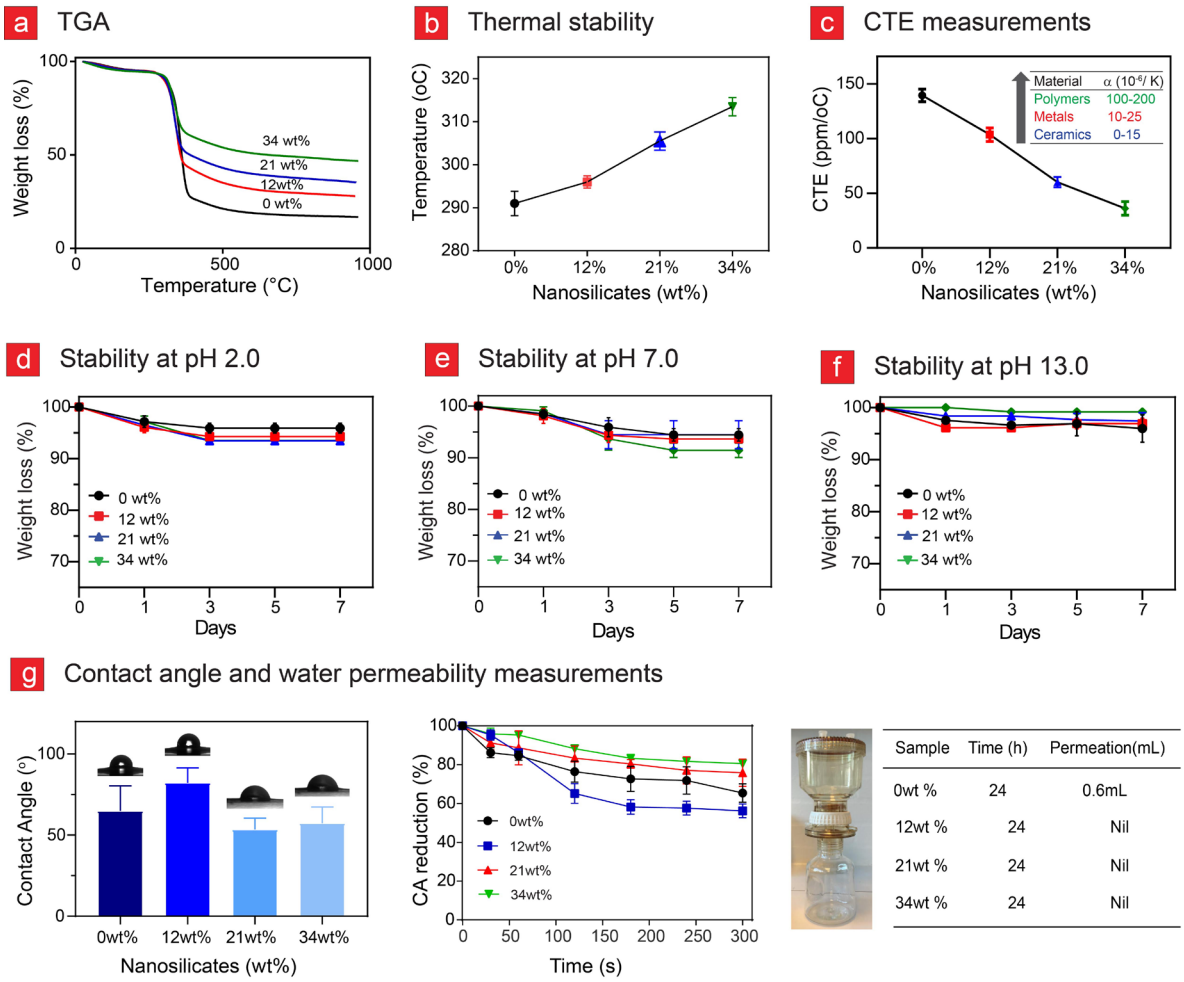

Sample	Time (h)	Permeation(mL)
0wt %	24	0.6mL
12wt %	24	Nil
21wt %	24	Nil
34wt %	24	Nil

Figure 4. Thermal, chemical stability and wettability characterization. (a) TGA, (b) Thermal stability and (c) CTE measurements. Stability studies in (d) pH 2.0, (e) pH 7.0 and (f) pH 13.0. (g) Static contact angle measurements, the percent-wise contact angle (CA) reduction at different time points and water permeability of Lapolose films.

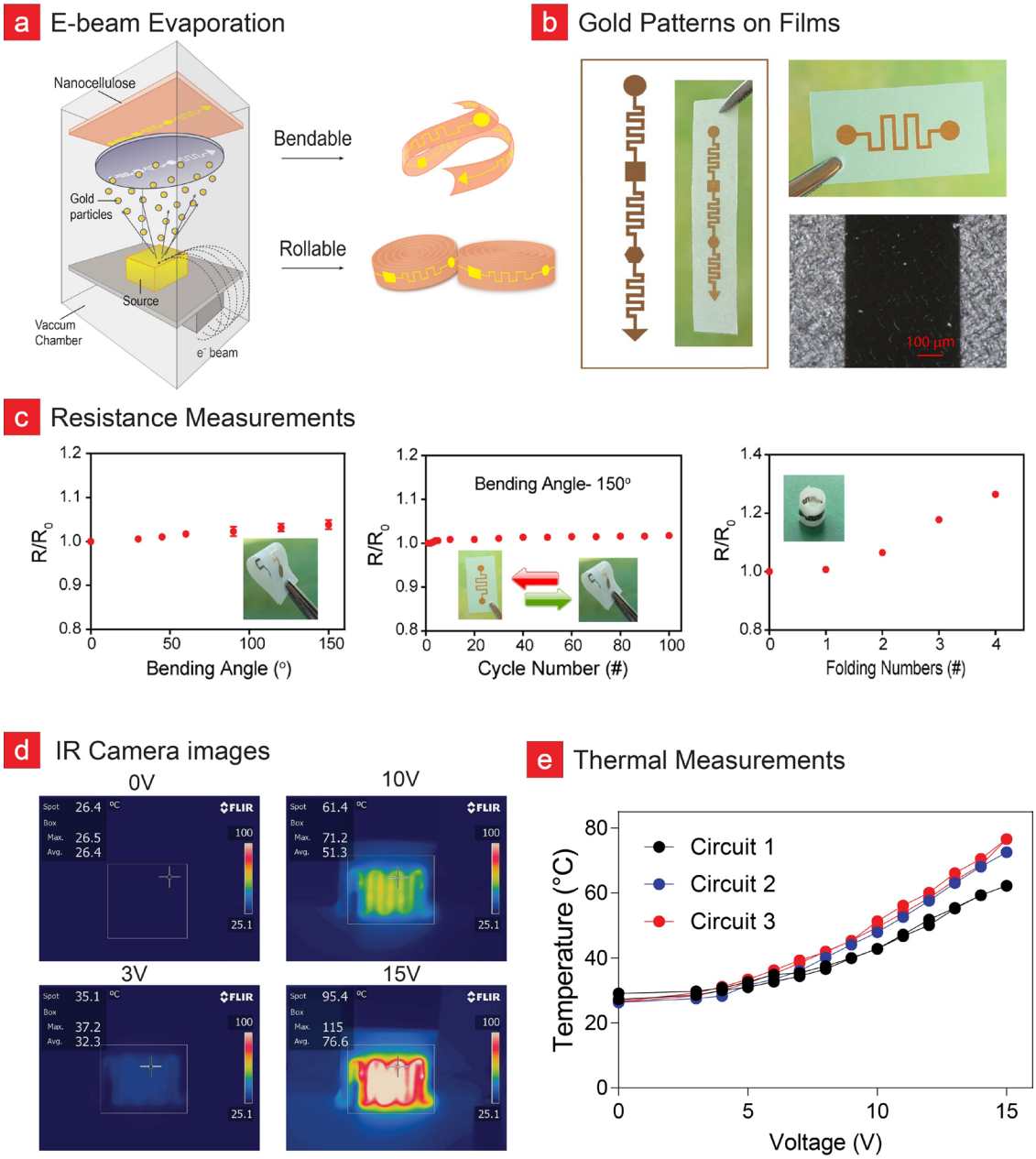

Figure 5. Flexible electronics and Joule heater development. (a) Schematic behind the fabrication process of the generated flexible electronics, (b) gold patterned Lapolose films, (c) resistance measurements as function of bending angle, bending cycle and number of folds, (d) IR images of the joule heater with respect to voltage and the corresponding (e) temperature variation.

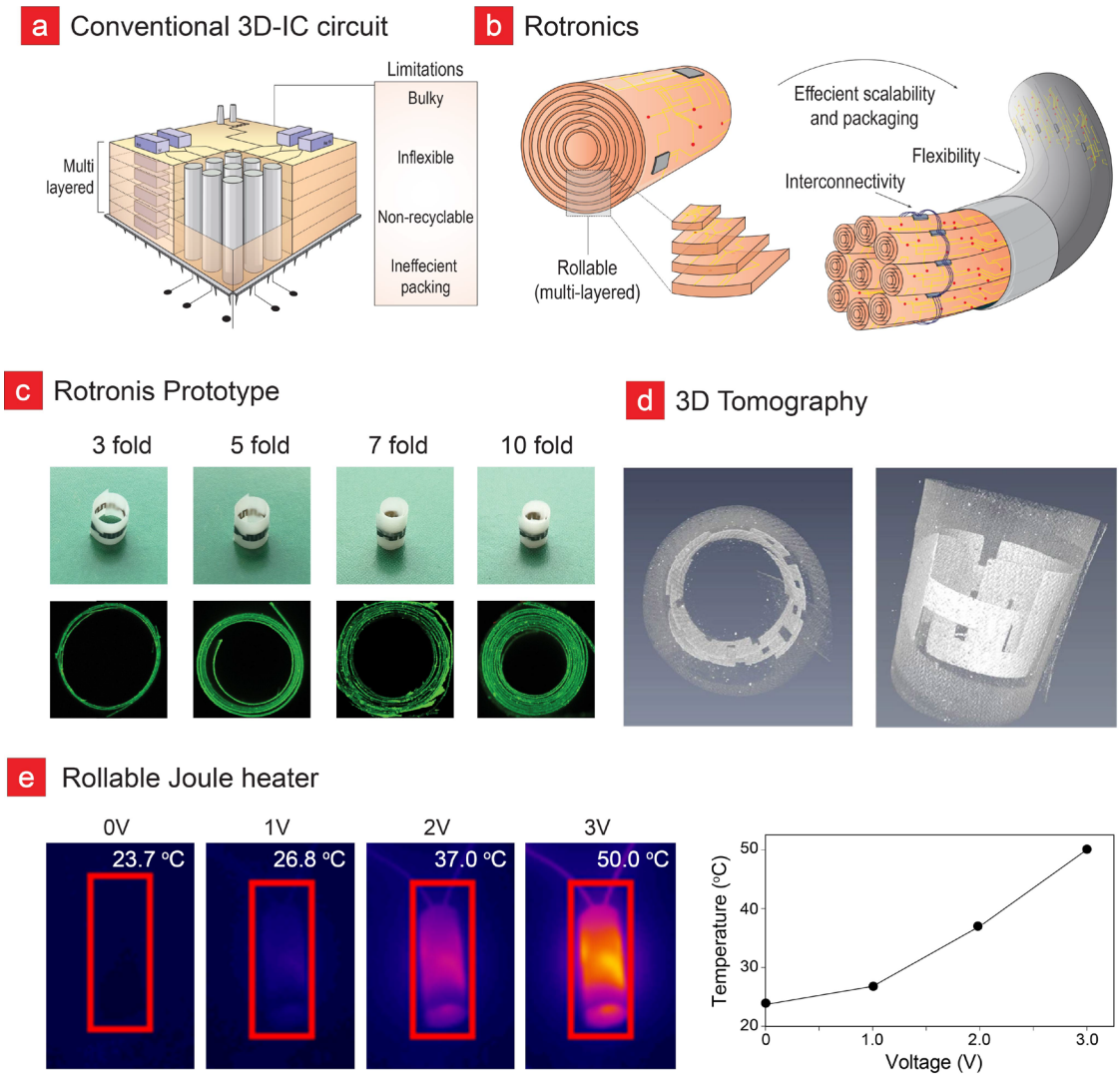

Figure 6. Three-dimensional-integrated circuits (3D-IC) from origami folding. (a) A conventional 3D-IC circuit based on rigid stacks that are connected through rigid and bulky silicon wires. (b) By rolling rollable electronics (rotronics) into cylinders and packing these cylinders into flexible wire-like configuration we have developed a simple, recyclable, efficient and low-cost alternative to today's conventional 3D-IC's. (c) A prototype rotronic device, which can fold up 10 folds without breaking and (d) 3D tomography of the 5 times folded rotronic device. (e) A 3D-IC joule heater and its corresponding IR camera images are shown here.

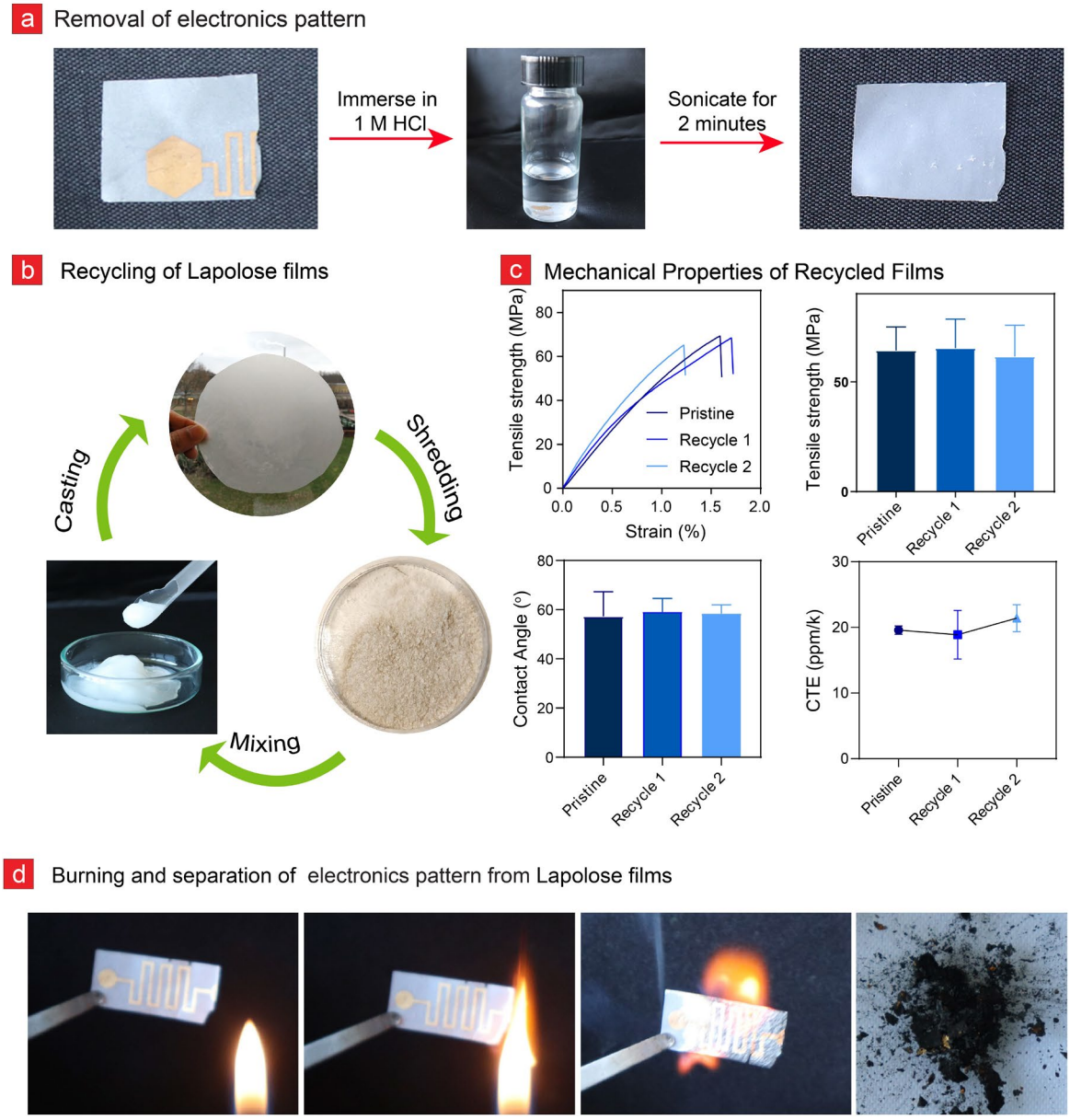

Figure 7. Recycling of Lapolose electronics. (a) Photographs showing the removable of gold patterns from the films. (b) The protocol behind the recycling process is depicted here. (c) Mechanical studies, water contact angle and CTE measurements of the films are studied after recycling. (d) Images showing how Lapolose electronics can be burned to separate electronics from the substrate.